Nuclear Theory'21
ed. V. Nikolaev, Heron Press, Sofia, 2002

Unified Description of Three Positive and Three Negative Parity Interacting Bands

A.A. Raduta[1] **and D. Ionescu**[2]

[1]Department of Theoretical Physics and Mathematics,
Bucharest University, POB MG11, Romania

[2]Department of Biophysics, Medical University "C. Davila", 76241, Bucharest, Romania

Abstract.

The coherent state model (CSM) is extended so that three negative parity bands are treated on equal footing with three positive parity bands. Calculations involve 6 structure coefficients and two deformation parameters which are fixed by a least square fitting procedure. Applications are made to ^{158}Gd, ^{172}Yb, ^{218}Ra, ^{226}Ra, ^{232}Th, ^{238}U, ^{238}Pu. A good agreement with the experimental data for excitation energies and transition probabilities is obtained. New signatures for octupole deformation, revealed in excited bands, are pointed out.

1 Introduction

The field of negative parity states is of about the same age as the one dealing with the positive parity states. The pioneering papers of this field appeared already in the beginning of the fifties [1,2]. They were based on high resolution alpha spectroscopy measurements. A sequence of states $1^-, 3^-, 5^-$ was identified through angular correlations and conversion coefficients analysis, as well by measuring the E1 branching ratio for the first state to 0^+ and 2^+. Also, it was concluded that these states belong to a $K^\pi = 0^-$ band. Since that early time, a lot of work has been devoted to this issue from both experimental and theoretical sides. The main achievements in this field of have been reviewed in several monographs [4,7]. In order to save space we shall not dwell on the history of this field and advise the reader to consult the two papers quoted above.

In the early stage of investigation, the negative parity states were considered as pure octupole vibrational states. Thus in a phenomenological language

they are determined by small oscillations of the nuclear surface parameterized by quadrupole and octupole shape variables around a spherical equilibrium shape. In the framework of a microscopic descriptions they are octupole particle-hole RPA (random phase approximation) states.

The interest in the field of negative parity states increased considerably when first suggestions for an octupole deformed nuclei appeared. Indeed, in Refs. [8,9] Chassman predicted parity doublets for several odd mass isotopes of Ac, Th and Pa. The doublet members have the same angular momentum, about the same energy but different parities. The lowest doublet constitutes a degenerate ground state, the degeneracy being caused by a reflection symmetry for the equilibrium shape. If the doublet is not mathematically degenerate but exhibits a small energy split, this is a sign of a reflection symmetry breaking. This assumption allowed for a consistent description of all available data for the low lying spectra of these isotopes.

On the other hand whenever a symmetry breaking appears a new behaviour for the many body system is expected. For example a rotational symmetry breaking by a quadrupole static deformation causes a rotational collective motion. Similarly the reflection symmetry breaking is associated to a static octupole deformation which is expected to determine new collective features for the nuclear system. Another theoretical work, which suggested that some even-even isotopes of Ra isotopes might have an octupole deformed ground band, belongs to Moller and Nix [10]. They showed that the binding energy of these nuclei gains about 2 MeV when in the mean field an octupole deformation is assumed.

The difficulty in the experimental study of pear shaped nuclei, is a missing observable which might be interpreted as a measure for the octupole deformation. Therefore some indirect information about this variable should be found.

Along the time several signatures were assigned to the octupole deformation: a) The low position of the state 1^- heading the band with $K^\pi = 0^-$ is an indication that, as function of the octupole deformation, the potential energy has a flat minimum. b) The parity alternating structure in the ground and the low 0^- bands suggests that the two bands may be viewed as being projected from a sole deformed intrinsic state, exhibiting both quadrupole and octupole deformations. If that is the case, the moments of inertia in the two bands are the same which results in obtaining a vanishing displacement energy function. c) A nuclear surface with quadrupole and octupole deformations might have the center of charge in a different position than the center of mass, which results in having a dipole moment which may excite the state 1^- from the ground state, with a large probability.

Here I shall talk about a phenomenological model proposed recently in Refs. [19, 20, 23] where we generalize the coherent state model (CSM) by assuming for the intrinsic states associated to the ground, beta and gamma bands also an octupole deformation. From each such a double deformed state, one projects

simultaneously the parity and angular momentum and consequently two bands of opposite parities are obtained. We want to see whether in the excited bands, $\beta^{\pm}, \gamma^{\pm}$ there are specific fingerprints of octupole deformation.

The plan of my talk is as follows. Since the formalism proposed for positive and negative bands, is based on CSM, we give a brief description of this formalism in Section 2. The CSM generalization, by including the octupole degrees of freedom, is performed in Section 3. Numerical results for ^{158}Gd, ^{172}Yb, ^{218}Ra, ^{226}Ra, ^{232}Th, ^{238}U, ^{238}Pu are discussed in Section 4. The main conclusions are summarized in Section 5.

2 Brief Review of the Coherent States Model for Three Interacting Bands

Two decades ago one of the present authors (A. A. R) proposed a phenomenological model to describe the main properties of the first three collective bands i.e., ground, beta and gamma bands [11,12]. The model space was generated through projection procedures from three orthogonal deformed states. The choice was made so that several criteria required by the existent data are fulfilled. The states are built up with quadrupole bosons and therefore we are dealing with those properties which are determined by the collective motion of the quadrupole degrees of freedom.

We suppose that the intrinsic ground state is described by coherent states of Glauber type corresponding to the zeroth component of the quadrupole boson operator $b_{2\mu}$. The other two generating functions are the simplest polynomial excitations of the intrinsic ground state, chosen in such a way that the mutual orthogonality condition is satisfied before and after projection. To each intrinsic state one associates an infinite rotational band. In two of these bands the spin sequence is $0^+, 2^+, 4^+, 6^+$, ..etc and therefore they correspond to the ground (the lowest one) and to the beta bands, respectively. The third one involves all angular momenta larger or equal to 2, and is describing, in the first order of approximation, the gamma band. The intrinsic states depend on a real parameter d which simulates the nuclear deformation. In the spherical limit, i.e. d goes to zero, the projected states are multi-phonon states of highest, second and third highest seniority, respectively. In the large deformation regime, conventionally called rotational limit (d equal to 3 means already a rotational limit), the model states behave like a Wigner function, which fully agrees the behavior prescribed by the liquid drop model. The correspondence between the states in the spherical and rotational limits is achieved by a smooth variation of the deformation parameter. This correspondence agrees perfectly with the semi-empirical rule of Sheline [13] and Sakai [14], concerning the linkage of the ground, beta and gamma band states and the member of multi-phonon states from the vibrational limit. This property is very important when one wants to describe the gross features of the reduced probabilities for the intra and inter bands transitions.

In this restricted collective model space an effective boson Hamiltonian is constructed. A very simple Hamiltonian was found, which has only one off-diagonal matrix element, namely that one connecting the states from the ground and the gamma bands.

$$H_{CSM} = H_2' + \lambda \hat{J}_2^2;\ H_2' = A_1(22\hat{N}_2 + 5\Omega_{\beta'}^{\dagger}\Omega_{\beta'}) + A_2\Omega_{\beta}^{\dagger}\Omega_{\beta}, \tag{2.1}$$

where $\hat{N}_2$ denotes the quadrupole boson number operator

$$\hat{N}_2 = \sum_{-2\leq m\leq 2} b_{2m}^{\dagger} b_{2m} \tag{2.2}$$

while $\Omega_{\beta'}^{\dagger}$ and $\Omega_{\beta}^{\dagger}$ stand for the following scalar polynomials:

$$\Omega_{\beta'}^{\dagger} = (b_2^{\dagger}b_2^{\dagger})_0 - \frac{d^2}{\sqrt{5}},\ \Omega_{\beta}^{\dagger} = (b_2^{\dagger}b_2^{\dagger}b_2^{\dagger})_0 + \frac{3d}{\sqrt{14}}(b_2^{\dagger}b_2^{\dagger})_0 - \frac{d^3}{\sqrt{70}} \tag{2.3}$$

The angular momentum carried by the quadrupole bosons, is denoted by $\hat{J}_2$. The boson states space is spanned by the projected states:

$$\phi_{JM}^{(i)} = N_J^{(i)} P_{MK}^J \psi_i,\ i = g, \beta, \gamma, \tag{2.4}$$

where the intrinsic states are:

$$\psi_g = e^{d(b_{20}^{\dagger} - b_{20})}|0\rangle,\ \psi_\beta = \Omega_\beta^{\dagger}\psi_g,\ \psi_\gamma = \Omega_\gamma^{\dagger}\psi_g. \tag{2.5}$$

where the excitation operator $\Omega_{\beta}^{\dagger}$ was defined above, while the operator which excites the gamma band states is:

$$\Omega_{\gamma}^{\dagger} = (b_2^{\dagger}b_2^{\dagger})_{22} + d\sqrt{\frac{2}{7}}b_{22}^{\dagger}. \tag{2.6}$$

The eigenvalues of the effective Hamiltonian in the restricted space of projected states have been analytically studied in both spherical and rotational limit. Compact formulae for transition probabilities in the two extreme limits have been also derived. This model has been successfully applied for a large number of nuclei from transitional and well deformed regions. It is worth to mention that by varying the deformation parameter and the parameters defining the effective Hamiltonian one can realistically describe nuclei satisfying various symmetries like, SU(5) (Sm region) [15], O(6) (Pt region) [11, 12], SU3 (Th region) [18], triaxial rotor (Ba, Xe isotopes) [16]. This model has been extended by including the coupling to the individual degrees of freedom [17]. In this way the spectroscopic properties in the region of back-bending were quantitatively described.

3 Simultaneous Description of Positive and Negative Parity Bands

Here we generalize the CSM formalism by assuming that the intrinsic ground state exhibits not only a quadrupole deformation but also an octupole one. Since the other bands, beta and gamma, are excited from the ground state, they have also this property. The octupole deformation of the intrinsic ground state is described by means of an axially symmetric coherent state for the octupole bosons $b^{\dagger}_{30}$. Thus the intrinsic states for ground, beta and gamma bands are:

$$\Psi_g = e^{f(b^{\dagger}_{30}-b_{30})}e^{d(b^{\dagger}_{20}-b_{20})}|0\rangle_{(3)}|0\rangle_{(2)},\ \Psi_\beta = \Omega^{\dagger}_{\beta}\Psi_g,\ \Psi_\gamma = \Omega^{\dagger}_{\gamma}\Psi_g. \quad (3.1)$$

The notation $|0\rangle_{(k)}$ stands for the vacuum state of the 2^k-pole boson operators. Note that any of these states is a mixture of positive and negative parity states. Therefore they don't have good reflection symmetry. Due to this feature the new extension of the CSM formalism has to project out not only the angular momentum but also the parity.

The intrinsic states of good parity are obtained by applying the operator $P^{(k)}$ on the $\Psi_i, i = g, \beta, \gamma$.

$$\Psi^{(k)}_i = P^{(k)}\Psi_i,\ i = g, \beta, \gamma,\ k = \pm \quad (3.2)$$

The member states of ground, beta and gamma bands are projected from the corresponding intrinsic states.

$$\begin{aligned}\varphi^{(i,k)}_{JM} =& \mathcal{N}^{(i,k)}_J P^J_{MK_i}\Psi^{(k)}_i,\ K_i = 2\delta_{i,\gamma},\ k = \pm; i = g, \beta\gamma \\ J =& (\delta_{i,g} + \delta_{i,\beta})(even\delta_{k,+} + odd\delta_{k,-}) + \delta_{i,\gamma}(J \geq 2).\end{aligned} \quad (3.3)$$

It can be shown that these projected states can be expressed by means of the octupole factor projected states and the projected states characterizing the CSM formalism.

$$\varphi^{(i,k)}_{JM} = \mathcal{N}^{(i,k)}_J \sum_{J_2,J_3}\left(N^{(k)}_{J_3}N^{(i)}_{J_2}\right)^{-1} C^{J_3\ J_2\ J}_{0\ 0\ 0}\left[\Psi^{(k)}_{J_3}\varphi^{(i)}_{J_2}\right]_{JM}. \quad (3.4)$$

Here $\mathcal{N}^{(i,k)}_J$ denotes the normalization factor.

An effective boson Hamiltonian will be studied in the restricted collective space generated by the six sets of projected states. Note that from each of the three intrinsic states, one generates by projection two sets of states, one of positive and one of negative parity. When the octupole deformation goes to zero, the resulting states are just those characterizing the CSM model. In this limit we know already the effective quadrupole boson Hamiltonian. When the quadrupole deformation is going to zero the system exhibits vibrations around an octupole deformed equilibrium shape. We consider for the octupole Hamiltonian a harmonic structure since the non-harmonic octupole terms can be simulated by the

quadrupole anharmonicities. As for the coupling between quadrupole and octupole bosons, we suppose that this can be described by a product between the octupole boson number operator, $\hat{N}_3$, and the quadruople boson anharmonic terms which are involved in the CSM Hamiltonian. Also, two scalar terms depending on the angular momenta carried by the quadrupole (J_2) and (J_3) octupole bosons, respectively are included. Note the including coupling terms with octupole factors different from $\hat{N}_3$, renormalizes the contribution of the coupling term already considered. Thus the model Hamiltonian has the expression:

$$\begin{aligned} H =& H_2' + \mathcal{B}_1\hat{N}_3(22\hat{N}_2 + 5\Omega^\dagger_{\beta'}\Omega_{\beta'}) + \mathcal{B}_2\hat{N}_3\Omega^\dagger_\beta\Omega_\beta \\ &+ \mathcal{B}_3\hat{N}_3 + \mathcal{A}_{(J23)}\vec{J}_2\vec{J}_3 + \mathcal{A}_J\vec{J}^2. \end{aligned} \tag{3.5}$$

As shown in Refs. [19–21] the coupling term $\vec{J}_2\vec{J}_3$ is necessary in order to explain the low position of the state 1^- in the even-even Ra isotopes. Indeed, this term is attractive in the state 1^- while for other angular momenta is repulsive.

Due to the specific structure of the CSM basis states the only non-vanishing off-diagonal matrix elements are those connecting the states of the ground and gamma and of the 0^- and 2^- bands, respectively. Energies of these bands are obtained by diagonalizing 2x2 matrices while for the remaining states are given as expected values on the corresponding projected states.

Energies depend on the structure coefficients $\mathcal{A}_k$ and $\mathcal{B}_k$, $(k = 1, 2, 3)$ defining the model Hamiltonian and the two deformation parameters, d and f. In the applications we consider here, the parameter $\mathcal{B}_2$ is not considered in the fitting procedure since data for the β^- band are missing. Therefore there are 8 parameters which are to be determined by fitting the data for excitation energies with the theoretical energies normalized to the ground state level. The eigenstates of the model Hamiltonian in the restricted space generated by the angular momentum and parity projected states are used to calculate the reduced probabilities for the E1, E2 and E3 transitions.

The transition operators are considered as lowest order polynomials in boson operators. Thus the E2 and E3 transition operators are linear in the quadrupole and octupole boson operators, respectively:

$$\begin{aligned} T_{1\mu} &= q_1 \sum_{\mu_2,\mu_3} C^{3\ 2\ 1}_{\mu_3\ \mu_2\ \mu}(b^\dagger_{3\mu_3} + (-)^\mu b_{3,-\mu_3})(b^\dagger_{2\mu_2} + (-)^\mu b_{2,-\mu_2}), \\ Q_{\lambda\mu} &= q_\lambda(b^\dagger_{\lambda\mu} + (-)^\mu b_{\lambda,-\mu}),\ \lambda = 2, 3. \end{aligned} \tag{3.6}$$

4 Numerical Results

The formalism described before, has been applied to seven even-even nuclei: ^{158}Gd, ^{172}Yb, ^{218}Ra, ^{226}Ra, ^{232}Th, ^{238}U, ^{238}Pu. Among these nuclei there are two, ^{218}Ra, ^{226}Ra, which are known to have octupole deformation. The negative parity states in the remaining nuclei have a vibrational character. Including

them in the present study, has the goal to prove the capacity of this model to describe the octupole deformation in the vanishing limit which results in providing an unified picture for spherical and octupole deformed nuclei. The results for the model parameters are listed in Table 1.

Table 1. The parameters defining the model Hamiltonian yielded by the fitting procedure are given in units of KeV. The deformation parameters d and f are adimensional.

	^{158}Gd	^{172}Yb	^{218}Ra	^{226}Ra	^{232}Th	^{238}U	^{238}Pu
d	3.00	3.68	1.40	3.15	3.25	3.90	3.90
f	0.30	0.30	0.30	0.65	0.30	0.60	0.30
$\mathcal{A}_1$	21.49	26.94	16.86	21.07	14.26	20.64	18.84
$\mathcal{A}_2$	-12.29	-17.68	-23.43	-17.41	-8.33	-9.72	-8.63
$\mathcal{A}_J$	3.10	4.72	1.81	0.51	2.26	1.55	2.23
$\mathcal{A}_{(J23)}$	34.70	38.49	18.09	9.53	11.93	20.45	10.77
$\mathcal{B}_1$	-11.84	-24.25	-7.13	-1.95	-6.17	-10.77	-8.39
$\mathcal{B}_3$	3 673.27	8 711.1	786.24	641.08	2 093.34	4 239.42	3 308.60

Inserting the parameters listed in Table 1 in Eqs. (3.12, 3.13) one obtains the excitation energies for the six rotational bands. Results are represented in Figures 1, 2. Energies are obtained with an octupole deformation which is relatively large for ^{226}Ra (0.8) and ^{238}U (0.6), and small, equal to 0.3, for the remaining ones. The three pairs of bands in ^{226}Ra have the specific feature that the doublet partners, starting from a certain angular momentum, have similar moments of inertia. Indeed, their energies are interleaved and lie on a curve which is close to a parabola. A very pronounced parity interleaved structure in beta bands can be seen in ^{158}Gd, ^{226}Ra and ^{232}Th. Except for ^{158}Gd, in gamma bands we have a typical case of parity doublets. Indeed, the states of equal angular momenta but different parity are almost degenerate. Deviations from this picture are observed for J$\geq$20 in ^{172}Yb, ^{238}U, 10$\leq J \leq$20 in ^{218}Ra and J$\leq$16 for ^{232}Th. The difference mentioned in gamma bands in different nuclei are determined by the fact that they are characterized by different quadrupole and octupole deformations. Note that the theoretical results for parity partner bands g$^{\pm}$, $\gamma^{\pm}$ in ^{158}Gd lie on almost parallel curves. In fact, this feature reclames equal moment of inertia in the partner bands but different zero points motion determined by the octupole intrinsic degrees of freedom.

A special attention should be paid to ^{232}Th. Indeed, for this nucleus we found 55 experimental excitation energies which were described with a reasonable small deviation. The energies of the two ground bands lie on different curves which intersect each other at high angular momentum (about 29^-). Beta bands reach each other much earlier, around J=12, and go together up to J=20 and then go apart. The gamma bands get similar moment of inertia (close J(J+1) patterns) starting with 20^+.

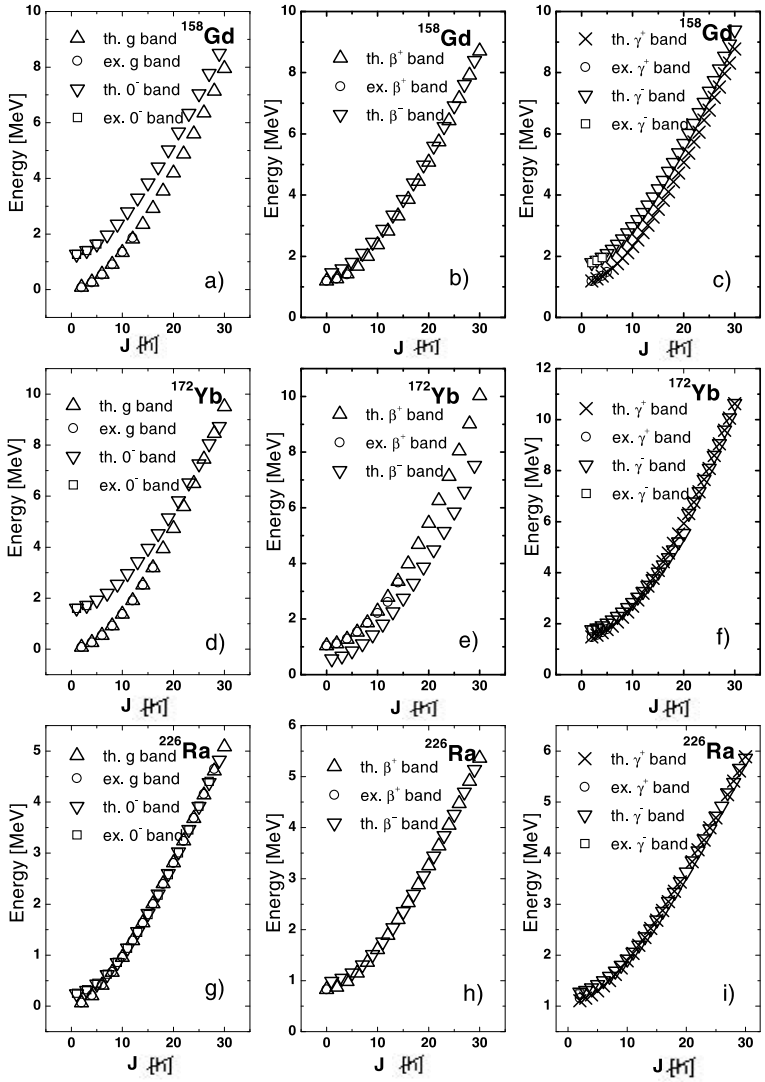

Figure 1. Predicted energies and available experimental data are given for several nuclei. Data are from are from [24–26] (^{158}Gd), [27–29] (^{172}Yb), [32, 33, 45](^{226}Ra)

It is worth mentioning that for ^{238}U, the calculated energies for the levels with J$\leq$9 in the second 0^- band are lower than those in the first 0^- band. Moreover, up to $J^\pi = 13^-$, the states belonging to the β^- band lie closer to the data in the observed 0^- band. In order to decide whether the experimental levels of $K^\pi = 0^-$

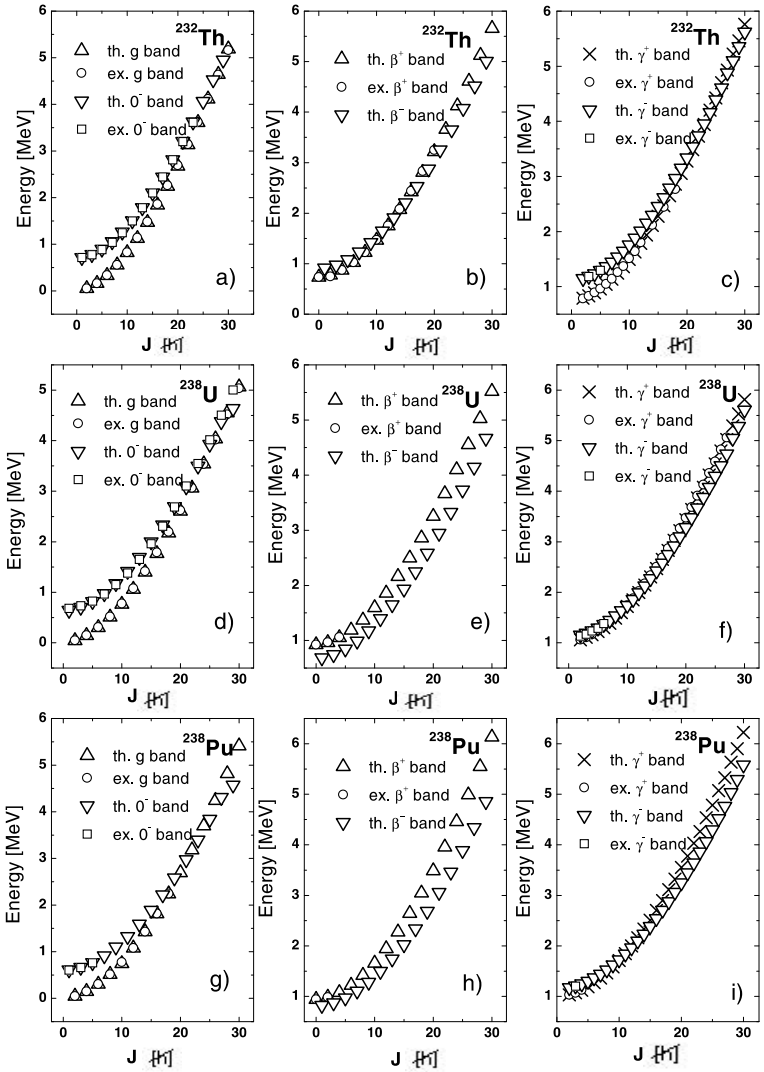

Figure 2. Predicted energies and available experimental data are given for several nuclei. Data are from are from [32, 34, 35] (^{232}Th), [36–38] (^{238}U), [34, 38, 39](^{238}Pu)

band belong, indeed, to the lowest rotational band it is necessary to have information about the E1 transitions to the ground band states.

From Figures 1 and 2, one easily sees that both ground and excited band energies behave nearly as a linear function of J(J+1). The larger the quadrupole deformation the smaller the deviation from this pattern. The only exception from

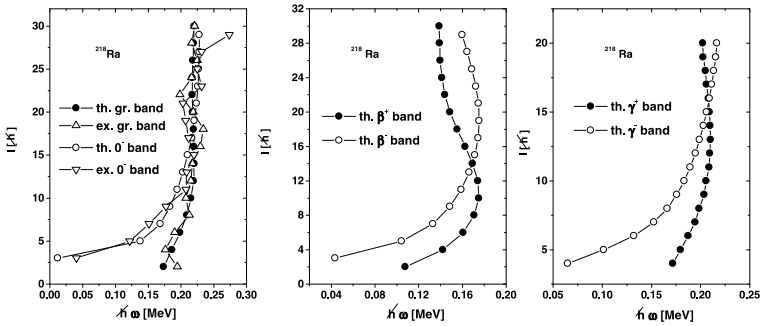

Figure 3. The angular momentum is plotted versus the rotational frequency for ground, 0^- (left panel), $\beta^{\pm}$ (middle panel) and $\gamma^{\pm}$ (right panel) bands of ^{218}Ra. The experimental data for positive and negative parity states are from [30, 31, 39] and are represented by up and down open triangles, respectively.

this feature is ^{218}Ra whose energies behave almost linearly on J. This case is represented separately in Figures 3 and 4 where the angular momentum is plotted versus the rotational frequency:

$$\hbar\omega_I = \frac{dE_I}{dI} \approx \frac{1}{2}(E_I - E_{I-2}). \tag{4.1}$$

Note that the curve for the ground band exhibits a back bending starting from J=16 and a forward bending from J=24$^+$. A double back bending is also seen for β^+ band. The remaining bands $g^-, \beta^-\gamma^{\pm}$, exhibit only a back bending.

The $E\lambda$ with $\lambda = 1, 2, 3$ transitions have been calculated by using the Eqs.(4.3-5). The negative parity states decay to the positive parity states of the

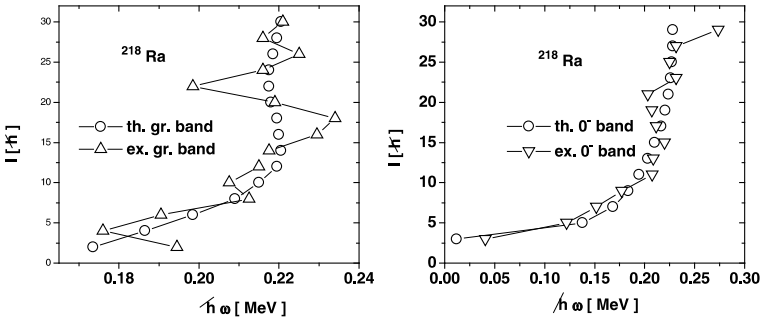

Figure 4. The angular momentum in the ground (left panel) and 0^- bands are plotted as function of the rotational frequency for ^{218}Ra. The corresponding experimental data are also given by up, for ground band, and down, for the band 0^-, open triangles.

partner band, by emitting E1 rays. The branching ratio

$$R_J = \frac{B(E1; J^- \to (J+1)^+)}{B(E1; J^- \to (J-1)^+)}. \tag{4.2}$$

seems to be sensitive to the angular momentum as well as to the specific structure of the nucleus under consideration. In Table 2, we give this ratio for ^{226}Ra where there are more available data for the ground band 0^-. Also we give the branching ratio characterizing the beta and gamma bands, respectively.

Table 2. The branching ratios given by Eq.(4.2) are given for the ground band of ^{226}Ra. Experimental data taken from Ref. [32, 40, 41] are given in the left column.

J^π	^{226}Ra		^{158}Gd		^{172}Yb		^{238}Pu	
	Exp.	Th.	Exp.	Th.	Exp.	Th.	Exp.	Th.
1^-	1.85± 1.20	1.84	1.8±0.2	1.64	2.4±0.6	1.76	1.8±0.05	1.78
3^-	0.87± 0.35	1.12	1.3±0.1	0.85	1.2±0.1	0.99	1.0± 0.10	1.02
7^-	1.79±1.59	0.86		0.47		0.62		0.66
9^-	1.27±0.68	0.83		0.38		0.52		0.56
11^-	1.12±0.79	0.83		0.32		0.45		0.49
13^-	1.06±0.68	0.85		0.28		0.39		0.43

The predicted ratios for the ground 0^- band agree quite well with the corresponding data. It is remarkable that the ratios characterizing the β^- band, not given here, are very close to those for the ground 0^- band. As for the gamma band, for odd values of angular momentum the ratio is smaller than the one characterizing the transitions of states from ground band 0^-, carrying the same angular momentum. However, the ratio is rapidly increasing with J. For example for ^{226}Ra already at $J^\pi = 7^-$ it exceeds the ratio in the ground 0^- band. In gamma band the state J^- might perform a E1 transition also to the state J^+. The ratio of this transition and the transition to $(J-1)^+$ is decreasing with J. As shown in Ref. [5], the ratio of intrinsic dipole and quadrupole moments in $K = 0$ bands can be related to the ratio of the E1 and E2 transitions:

$$|\frac{D_0}{Q_0}| = \left[\frac{5(I-1)}{8(2I-1)}\frac{B(E1; I \to (I-1))}{B(E2; I \to (I-2))}\right]^{1/2}. \tag{4.3}$$

This equation is derived by using the symmetric rotor expression for the transitions involved. Inserting the predicted values for the B(E1) and B(E2) values, one obtains predictions for the ratio of intrinsic moments. Possible deviations from the corresponding experimental values may reflect the deviation of the present formalism from the symmetric rotor picture [22]. Since the square root from the above equation is proportional to the ratio of the dipole and quadrupole effective charges q_1/q_2, which are not known in the present work, we fixed this

Table 3. The ratio $|D_0/Q_0|$ for the ground and β bands is given for negative parity states of ^{226}Ra. Theoretical predictions, right column, are compared with the corresponding data extracted from Ref. [45], given in the first column. Data are presented in units of $10^{-4}\ fm^{-1}$.

I^π	g band		β band
	Exp.	Th.	Th.
3^-		2.41	1.52
5^-		2.47	1.56
7^-		2.52	1.59
9^-	2.57 ± 0.20	2.57	1.61
11^-	2.50 ± 0.14	2.60	1.64
13^-	1.96 ± 0.15	2.64	1.66
15^-	2.50 ± 0.50	2.67	1.68
17^-	2.49	2.70	1.70
19^-		2.73	1.73

ratio so that the prediction for 7^- fits the experimental value for $|D_0/Q_0|$. The results for ^{226}Ra are compared with experimental data in Table 3, for the $K^\pi = 0^-$ ground and beta bands.

We remark a good agreement between predicted and experimental results for ground band. Although in the rotational limit the ratio $|D_0/Q_0|$ for ground and beta bands should be the same, in the present model the ratio for beta band is smaller than that for ground band.

The transition operator for the E2 transitions is given by Eq.(3.6). The effective charge is fixed so that the experimental B(E2) value for the transition

Table 4. Reduced transition probabilities, $B(E2; J^+ \to J'^+)$, for positive ground and β bands in ^{226}Ra, given in units of e^2b^2. Data are extracted from Ref. [45].

J^+/J'^+	J^+			$(J+2)^+$		
	g band		β band	g band		β band
	Exp.	Th.	Th.	Exp.	Th.	Th.
0^+				5.14	5.14	5.96
2^+	$0.43^{+0.19}_{-0.17}$	1.46	1.70	$2.73^{+0.13}_{-0.07}$	2.68	3.10
4^+	$1.26^{+0.35}_{-0.24}$	1.33	1.54	$2.59^{+0.06}_{-0.07}$	2.43	2.79
6^+	$2.56^{+0.33}_{-0.66}$	1.30	1.50	$2.25^{+0.05}_{-0.08}$	2.37	2.70
8^+	$1.88^{+0.90}_{-0.18}$	1.29	1.48	$2.05^{+0.16}_{-0.07}$	2.38	2.69
10^+	$1.13^{+0.67}_{-0.23}$	1.29	1.47	$3.85^{+0.18}_{-0.31}$	2.42	2.72
12^+	$1.06^{+0.62}_{-0.74}$	1.28	1.46	$2.14^{+0.29}_{-0.12}$	2.48	2.77
14^+		1.28	1.45	$2.32^{+1.07}_{-0.35}$	2.55	2.82
16^+		1.27	1.44	$0.94^{+0.25}_{-0.20}$	2.63	2.89

Table 5. The reduced transition probabilities $B(E2; J^- \rightarrow J'^-)$, for negative ground and β bands, given in units of e^2b^2 for ^{226}Ra. Data are extracted from Ref. [45].

J^-/J'^-	J^-			$(J+2)^-$		
	g band		β band	g band		β band
	Exp.	Th.	Th.	Exp.	Th.	Th.
1^-	$5.74^{+0.69}_{-0.97}$	2.05	2.37	$4.46^{+0.14}_{-0.23}$	3.09	3.58
3^-	$2.92^{+1.42}_{-0.77}$	1.36	1.58	$2.39^{+0.05}_{-0.12}$	2.49	2.86
5^-	$2.11^{+0.53}_{-0.38}$	1.32	1.52	$1.50^{+0.02}_{-0.05}$	2.34	2.69
7^-	$2.36^{+0.56}_{-1.17}$	1.30	1.49	$1.98^{+0.02}_{-0.12}$	2.31	2.64
9^-	$2.41^{+1.03}_{-0.81}$	1.29	1.48	$2.41^{+0.21}_{-0.50}$	2.33	2.64
11^-		1.28	1.47	$4.35^{+0.95}_{-0.61}$	2.38	2.68
13^-		1.27	1.46	$3.48^{+2.15}_{-1.58}$	2.45	2.73

$0^+ \rightarrow 2^+$ is reproduced. Results for ^{226}Ra are collected in Tables 4 and 5. We note that transitions in beta bands are in general stronger than in ground bands.

The results for octupole transitions between parity partner bands $g^{\pm}$, are given in Table 6 for ^{226}Ra. The octupole effective charge is chosen so that the experimental B(E3) value for the transition $0^+_g \rightarrow 3^-_g$ is reproduced. Again the agreement with the data is fairly good.

Table 6. Reduced transition probabilities $B(E3; J^+ \rightarrow J'^-)$ for ground band of ^{226}Ra, given in units of e^2b^3. The effective charge was fixed so that the experimental B(E3) value for the transition $0^+ \rightarrow 3^-$ is reproduced. Experimental data are from Ref. [45].

J^+/J'^-	$(J-3)^-$		$(J-1)^-$		$(J+1)^-$		$(J+3)^-$	
	Exp.	g	Exp.	g	Exp.	g	Exp.	g
0^+							$1.17^{+0.06}_{-0.06}$	1.17
2^+			$0.28^{+0.01}_{-0.03}$	0.27	$0.26^{+0.07}_{-0.07}$	0.29	$0.80^{+0.05}_{-0.05}$	0.60
4^+	$0.24^{+0.05}_{-0.02}$	0.18	$0.23^{+0.10}_{-0.04}$	0.18	> 0.32	0.24	$0.67^{+0.04}_{-0.07}$	0.54
6^+	$0.52^{+0.20}_{-0.20}$	0.22	$0.30^{+0.09}_{-0.09}$	0.17	$0.44^{+0.52}_{-0.15}$	0.23	$0.65^{+0.04}_{-0.09}$	0.53
8^+	> 0.34	0.24		0.17		0.22	$0.28^{+0.15}_{-0.44}$	0.54

5 Conclusions

In this lecture I have described the basic ideas of a phenomenological description of six rotational bands, three of positive and three of negative parities. These bands are organized in three pairs $g^{\pm}, \beta^{\pm}, \gamma^{\pm}$, each pair being generated by projection from a quadrupole and octupole deformed state. The intrinsic functions

have not good reflection symmetry and therefore the parity projection distinguishes between partner bands.

Many features seen in ground and the lowest $K^\pi = 0^-$ bands, customarily considered as signatures for an octupole deformation, are also seen in the other two pairs of bands called $\beta^\pm$ and $\gamma^\pm$ bands, respectively. Moreover several new properties, specific for the excited bands, were pointed out.

Partner bands intersect each other or have common J(J+1) pattern for a finite interval of angular momentum. For the angular momenta where the two energy functions are represented by similar curves, the nucleus under consideration is supposed to be octupole deformed.

Several specific properties of β^- band, have been pointed out. Indeed, there are nuclei like ^{238}U, ^{238}Pu, ^{172}Yb, where the band β^- is lower in energy than the parity partner band, β^+. The negative parity beta band can intersect also the ground negative band.

For pear shaped nuclei, the most interesting features are provided by the $\gamma^\pm$ bands. Indeed, the two bands are the only partner bands having a similar spin sequence. Therefore for weakly octupole deformed nuclei, in these bands one may identify parity doublet states, i.e. states of the same angular momenta, the same energy but of different parities.

The comparison of the calculated excitation energies with the available corresponding data is very good. To get an idea about the quality of the agreement obtained, we mention the case of ^{232}Th where 55 experimental energy levels are described with a deviation of at most 20 KeV.

The electric transition properties were calculated mainly for ^{226}Ra were there are some relevant experimental data. The agreement of the theoretical results with the experimental data is reasonable good.

As a final conclusion, the results I presented here and described in extenso in Ref. [23] are obtained within a formalism which treats in an unified fashion the positive and negative parity bands. In the near future we shall atempt to enlarge the number of band pairs by adding the ones with $K^\pi = 1^\pm$.

References

[1] F. Asaro, F.S. Stephen and I. Perlman, (1953) *Phys. Rev.* **92** 1495.

[2] F.S. Stephen, Jr., F. Asaro and I. Perlman,(1955) *Phys. Rev.* **100** 1543.

[3] S. G. Rohozonski, (1988) *Rep. Prog. Phys.* **51** 541.

[4] I. Ahmad and P. A. Butler, (1993) *Annu. Rev. Nucl. Part. Sci.* **43** 71.

[5] P.A. Butler and W. Nazarewicz, (1996) *Rev. Mod. Phys.* **68** 349.

[6] S. Frauendorf, (2001) *Rev. Mod. Phys.* **73** 463.

[7] P. A. Butler and W. Nazarewicz, (1991) *Nucl. Phys.* **A533** 249.

[8] R. R. Chasman, (1979) *Phys. Rev. Lett.* **42** 630.

[9] R. R. Chasman, (1980) *Phys. Lett* **B96** 7.

[10] P. Moller and J. R. Nix, (1981) *Nucl. Phys.* **A361** 117.
[11] A. A. Raduta *et al*, (1981) *Phys. Lett.* **B99** 444.
[12] A. A. Raduta *et al*, (1982) *Nucl. Phys.* **A381** 253.
[13] R. K. Sheline, (1960) *Rev. Mod. Phys.* **32** 1.
[14] M. Sakai, (1967) *Nucl. Phys.* **A104** 301; (1970) *Nucl. Data Tables* **A8** 323; (1972) **A10** 511.
[15] A. A. Raduta and N. Sandulescu, (1986) *Rev. Roum. Phys.* **31** 765.
[16] U. Mayer, A. A. Raduta, A. Faessler, (1998) *Nucl. Phys.* **A637** 321.
[17] A. A. Raduta, C. Lima, A. Faessler, (1983) *Phys. Lett.* **B121** 1; (1987) *Z. Phys.* **A327** 275.
[18] A. A. Raduta and C. Sabac, (1983) *Ann. Phys.*(NY) **148** 1.
[19] A. A. Raduta, Al. H. Raduta, A. Faessler, (1997) *Phys. Rev*. **C55** 1747.
[20] A. A. Raduta, Al. H. Raduta, A. Faessler, (1997) *J. Phys.* **G23** 149.
[21] A. A. Raduta, A. Faessler, R. K. Sheline, (1998) *Phys. Rev.* **C57** 1512.
[22] A. Ya. Dzyublik and V. Yu. Denisov, (1993) *Phys. At. Nucl.* **56** 30.
[23] A. A. Raduta, D. Ionescu, A. Faessler, (2002) *Phys. Rev.* **C65** 064322.
[24] M. Sugawara *et al.*, (1993) *Nucl. Phys.* **A557** 653c.
[25] M. A. Lee, (1989) *Nucl. Data Sheets* **56** 199.
[26] R. Bloch, B. Elbek and P. O. Tjom, (1967) *Nucl. Phys.* **A91** 576.
[27] J. R. Gresswell *et al*, (1981) *J. Phys.* **G7** 235.
[28] D. G. Burke and B. Elbek, (1967) *Mat. Fys. Medd. Dansk. Vid. Selsk.* **36** 6.
[29] Singh Balraj, (1995) *Nucl. Data Sheets* **75** 199.
[30] N. Schulz *et al*, (1989) *Phys. Rev. Lett.* **63** 2645.
[31] Y. Gono *et al*., (1986) *Nucl. Phys.* **A459** 427.
[32] J. F. G. Cocks *et al.*, (1999) *Nucl. Phys.* **A645** 63.
[33] Y. A. Ellis-Akovali, (1993) *Nucl. Data Sheets* **69** 155.
[34] R. S. Simon *et al*., (1982) *Phys. Lett.* **B108** 449.
[35] E. Grosse *et al*, (1975) *Phys. Rev. Lett.* **35** 565.
[36] D. Ward *et al.*, (1996) *Nucl. Phys.* **A600** 88.
[37] J. G. Alessi *et al*, (1981) *Phys. Rev.* **C23** 79.
[38] E. N. Shurshikov, (1988) *Nucl. Data Sheets* **53** 601.
[39] M. Gai *et al.*, (1983) *Phys. Rev. Lett.* **51** 646.
[40] J. F. Smith *et al*.,(1995) *Phys. Rev. Lett.* **75** 1050.
[41] J. F. C. Cocks *et al.*, (1997) *Phys. Rev. Lett.* **78** 2920.
[42] R. C. Greenwood *et al.*, (1978) *Nucl. Phys.* **A304** 327.
[43] R. C. Greenwood *et al.*, (1975) *Nucl. Phys.* **A252** 260.
[44] C. M. Lederer, (1981) *Phys. Rev.* **C24** 1175.
[45] H. J. Wollershein *et al.*, (1993) *Nucl. Phys.* **A556** 261.